FEBS Letters

FEBS PRESS science publishing by scientists

Small-molecule stabilization of the p53 – 14-3-3 protein-protein interaction

Richard G. Doveston[1], Ave Kuusk[1,2], Sebastian A. Andrei[1], Seppe Leysen[1], Qing Cao[3,†], Maria P. Castaldi[3], Adam Hendricks[3], Luc Brunsveld[1], Hongming Chen[2], Helen Boyd[2] and Christian Ottmann[1,4]

1 Laboratory of Chemical Biology, Department of Biomedical Engineering and Institute for Complex Molecular Systems, Eindhoven University of Technology, The Netherlands
2 Discovery Sciences, Innovative Medicines and Early Development Biotech Unit, AstraZeneca R&D Gothenburg, Mölndal, Sweden
3 Discovery Sciences, Innovative Medicines and Early Development Biotech Unit, AstraZeneca, Waltham, MA, USA
4 Department of Chemistry, University of Duisburg-Essen, Germany

Correspondence
C. Ottmann, Laboratory of Chemical Biology, Department of Biomedical Engineering, Institute for Complex Molecular Systems, Eindhoven University of Technology, P.O. Box 513, 5600 MB Eindhoven, The Netherlands
Tel: +31 40 247 2835
E-mail: c.ottmann@tue.nl
and
H. Boyd, Discovery Sciences, Innovative Medicines and Early Development Biotech Unit, AstraZeneca R&D Gothenburg, Pepparedsleden 1, 431 83 Mölndal, Sweden
Tel: +46 31 776 1749
E-mail: helen.boyd@astrazeneca.com

†Present address
RA Pharmaceuticals Inc., 87 Cambridge Park Drive, Cambridge, MA 02140, USA

(Received 17 February 2017, revised 1 June 2017, accepted 14 June 2017, available online 6 August 2017)

doi:10.1002/1873-3468.12723

Edited by Michael Bubb

14-3-3 proteins are positive regulators of the tumor suppressor p53, the mutation of which is implicated in many human cancers. Current strategies for targeting of p53 involve restoration of wild-type function or inhibition of the interaction with MDM2, its key negative regulator. Despite the efficacy of these strategies, the alternate approach of stabilizing the interaction of p53 with positive regulators and, thus, enhancing tumor suppressor activity, has not been explored. Here, we report the first example of small-molecule stabilization of the 14-3-3 – p53 protein-protein interaction (PPI) and demonstrate the potential of this approach as a therapeutic modality. We also observed a disconnect between biophysical and crystallographic data in the presence of a stabilizing molecule, which is unusual in 14-3-3 PPIs.

Keywords: 14-3-3 proteins; fluorescence polarization; isothermal titration calorimetry; p53; PPI stabilization; protein crystallography

The tumor suppressor protein p53 plays a critical role in the regulation of a number of genes with functions associated to DNA repair, cell cycle arrest and apoptosis [1]. Mutations to this transcription factor render it inactive in over 50% of all cancers and thus the p53 pathway has become an important therapeutic target [2]. One significant approach has been to target mutant p53 and restore the wild-type tumor suppression

Abbreviations
CTD, C-terminal domain; FC-A, fusicoccin A; FP, fluorescence polarization; ITC, isothermal titration calorimetry; PPI, protein-protein interaction.

function [3–5]. However, the major small molecule-based strategy for activating wild-type p53 function has been centered on inhibition of the p53 interaction with its primary negative regulator, MDM2. This approach has had considerable success, with a number of compounds progressing to clinical trials [2,6]. Despite this, the modulation of other protein-protein interactions (PPI) in the p53 interactome has received little attention.

The 14-3-3 family of proteins are a class of dimeric adapter proteins with seven isoforms in humans (β, γ, ε, η, σ, τ, ζ). They play a diverse set of roles within the cell including cell-cycle control, signal transduction, apoptosis and protein trafficking or sub-cellular localization [7]. 14-3-3 proteins exert their function through binding of several hundred partner proteins usually bearing a phosphorylated binding motif and many of which are involved in human disease [8]. The modulation of 14-3-3 PPIs has been widely demonstrated [9,10], but in particular the stabilization of interactions with partner proteins by the natural product fusicoccin A (FC-A; Fig. 1A) and derivatives is significant [11]. In this context stabilization is defined as an increased binding affinity (as shown by a reduced K_d) between protein and partner protein peptide mimic as a direct result of small-molecule binding at the PPI interface. This 'molecular glue' stabilizing effect is most pronounced with binding partners bearing a C-terminal 14-3-3 recognition motif, or 'mode 3' motif (Fig. 1C) – clinically important examples include ERα [12], human protein glycoprotein (GP)Ibα [13] and TASK3 [14]. More recently it has been shown that fusicoccane derivatives can also stabilise internal or 'mode 1 or 2' partner protein recognition motifs. For example FC-A has been shown to stabilize the 14-3-3 interaction with CFTR [15], the semi-synthetic derivative ISIR-005 stabilizes the interaction with Gab2 [16] and related natural product cotylenin the interaction with C-Raf [17].

14-3-3 proteins act as positive regulators of p53 through binding to the disordered C-terminal domain (CTD) following stress-induced phosphorylation of key residues (Ser378, Ser366 or Thr387) [18–20]. This important PPI network consists of a number of 14-3-3 isoform-specific functions. The σ isoform has been shown to positively regulate p53 in cells and supress tumor growth, presumably by antagonising MDM2-mediated ubiquitination of p53 [18]. The γ and ε isoforms have been linked with enhanced p53 tetramerization and thus transcriptional activity [19,20]. A recent study also reported the negative regulation of 14-3-3γ as a result of downstream p53 transcriptional activity and further highlights the complexity of the network [21]. Never-the-less the stabilization of the p53 – 14-3-3σ PPI represents a highly attractive, if challenging, drug discovery strategy.

In 2010 our Group reported the crystal structure of 14-3-3σ bound to the extreme C-terminus of p53 (9 amino acid residues) with phosphorylation at Thr387 [22]. This provided a structural basis for 14-3-3σ binding to p53 which occurs *via* a recognition motif that is distinct from the classical 'mode 1, 2 or 3' model

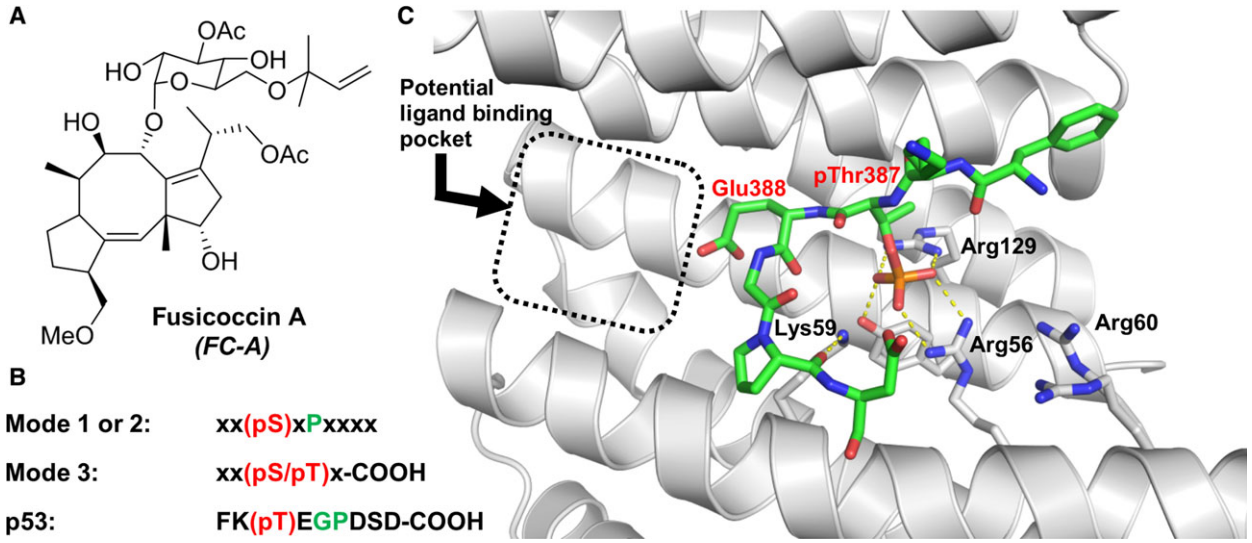

Fig. 1. (A) Structure of fusicoccin A (FC-A). (B) Comparison of 14-3-3 partner protein binding motifs: Mode 1 and 2, mode 3 and p53. Phosphorylated residues are shown in red and key proline/glycine residues in green. (C) Binary crystal structure showing a p53-CTD 9mer peptide (pThr387, coloured according to atom with red residue labels) bound to 14-3-3σ (grey with black residue labels). The potential ligand binding pocket is identified. (3LW1: wwpdb.org).

(Fig. 1B). In this case Gly followed by Pro at +2 and +3 residues C-terminal to the phosphorylated Thr387 cause the peptide to fold back on itself and as a result form a potential ligand binding pocket at the interaction interface (Fig. 1C). However, it was hypothesised that the Glu388 side-chain that is orientated directly into that space would prevent interface binding of, and thus stabilization by, fusicoccane derivatives [22]. Since then, enhancement of the 14-3-3σ – p53 interaction by amifostine, a radioprotector in its dephosphorylated form, has been demonstrated in a cellular and radiative-independent context although there is as yet no chemical rationale for these observations [23].

Here, we report that FC-A does in fact act as a stabilizer of this important PPI despite the previous hypotheses to the contrary. This finding marks a significant milestone toward demonstrating proof-of-concept for targeting the p53 – 14-3-3σ interface as a therapeutic modality. However, our discovery is also met with a paradox that is highly unusual in the case of 14-3-3 proteins: Although the biophysical data clearly points to stabilization, crystallographic studies indicate greater disorder in the ternary complex. This could be explained as an artefact of crystal soaking but may also suggest that FC-A acts *via* an allosteric rather than a 'molecular glue' mode-of-action in this case.

Materials and methods

Peptide synthesis

Thr387 p53 CTD phosphopeptides were either obtained from commercial sources (TAMRA-32mer and 12mer for crystallography) or prepared in-house by Fmoc solid phase peptide synthesis (15mer). Peptide sequences and sources are summarised in Table 1. Detailed synthetic procedures are described in the Supporting Information.

14-3-3 Expression and purification

His_6-tagged 14-3-3σ protein (full-length and ΔC) was expressed in NiCo21(DE3) competent cells with a pPROEX HTb plasmid, and purified using Ni^{2+}-affinity chromatography. The proteins were dialyzed against fluorescence polarization (FP) or isothermal titration calorimetry (ITC) buffer before usage. The ΔC variant for crystallization was treated with TEV-protease to cleave off the His_6-tag, followed by a second Ni^{2+}-affinity column and size exclusion chromatography.

Fluorescence polarization

Fluorescence polarization experiments were conducted in FP buffer (10 mM HEPES pH 7.5, 150 mM NaCl, 0.1% Tween20, 1.0 $mg{\cdot}mL^{-1}$ BSA) using fixed concentrations of TAMRA-labelled 32mer peptide (10 nM) and DMSO (1% v/v) in Corning black, round-bottom, low-binding 384-well plates. Plates were incubated at room temperature for 1 h before measuring polarization with a Tecan (Tecan Group Ltd., Männedorf, Switzerland) Infinite F500 plate reader (excitation: 535 nm; emission: 590 nm). FP data was analyzed in ORIGIN 2015 Sr2 (OriginLab Corporation, Northampton, MA, USA) and sigmoidal curves were fitted using the Levenburg-Marquardt iteration algorithm. Detailed procedures for 14-3-3σ titration and dose-response experiments are described in the Supporting Information.

Isothermal titration calorimetry

Isothermal titration calorimetry experiments were conducted using a Malvern MicroCal iTC_{200} (Malvern Instruments Ltd., Malvern, UK) instrument at 25 °C in ITC buffer (25 mM HEPES pH 7.5, 100 mM NaCl, 10 mM $MgCl_2$, 0.50 mM TCEP). 15mer peptide (1.0 mM) was titrated (2 × 18 injections of 2 μL) to 14-3-3σ (0.10 mM) in the cell. DMSO (1% v/v ± FC-A to a final concentration of 1.0 mM) was added to both cell and titrant. Data from the two titration series was merged using CONCAT32 software (Malvern Instruments Ltd). ORIGIN 7.0 (OriginLab Corporation) software was used for data analysis by a non-linear least squares routine using a single-site binding model with varying stoichiometry (N), association constant and molar binding enthalpy (ΔH). The data presented are representative of three replicates. For full experimental details and results see the Supporting Information.

Protein crystallisation and structure determination

Crystals of the binary complex of p53 and 14-3-3σ were grown by mixing 10 $mg{\cdot}mL^{-1}$ 14-3-3σΔC in a molar ratio of 1 : 1.5 with p53 12-mer C-terminal peptide in 20 mM Hepes pH 7.5, 2 mM $MgCl_2$ and 2 mM BME and

Table 1. Peptide sequences and sources.

Peptide	Sequence	Source
12mer	H_2N-KLMFK(pT)EGPDSD-COOH	Caslo
15mer	H_2N-RHKKLMFK(pT)EGPDSD-COOH	In-house
TAMRA-32mer	TAMRA-LC-SRAHSSHLKSKKGQSTSRHKKLMFK(pT)EGPDSD-COOH	Anaspec

incubating overnight at 277 K. The formed complex was then set up for crystallization by mixing 1 : 1 with 0.095 M HEPES pH 7.1, 26% PEG400, 0.19 M $CaCl_2$ and 5% glycerol at 277 K. Crystals grew within a week and were fished and directly flash cooled in liquid nitrogen before measuring.

For soaking of the crystals a 10 mM solution of FC-A in ethanol (2.0 μL) was pipetted on a crystallization plate and left to evaporate forming a thin FC-A layer. About 2.0 μL of equilibrated crystallization liquor was then pipetted on top of this layer and 14-3-3σΔC/p53 12-mer crystals were transferred into this new drop.

X-ray diffraction data was collected using an in-house Rigaku Micromax-003 (Rigaku Europe, Kemsing Sevenoaks, UK) sealed tube X-ray source and a Dectris Pilatus 200K detector (DECTRIS Ltd., Baden-Daettwil, Switzerland) at 100 K or at the DESY PETRAIII P11 synchrotron beamline (DESY, Hamburg, Germany). The data was indexed and integrated using iMosflm and scaled and merged using AIMLESS. Phasing was done by molecular replacement using PHASER (www.ccp4.ac.uk) and 3LW1 (wwpdb.org) as a starting model and was followed by iterative rounds of refinement and manual model building using PHENIX.REFINE (https://www.phenix-online.org) and COOT (https://www2.mrc-lmb.cam.ac.uk/personal/pemsley/coot/) respectively. Model validation was performed using MOLPROBITY (http://molprobity.biochem.duke.edu/) prior to PDB submission.

14-3-3σΔC/p53 12-mer CTD, 5MOC: wwpdb.org.
14-3-3σΔC/p53 12-mer CTD/FC-A, 5MXO: wwpdb.org.

For further details see the Supporting Information.

Results

Identification of FC-A as a stabilizer: fluorescence polarization

As part of a broad search for stabilizer molecules we developed a robust FP assay suitable for medium to high-throughput screening of compound libraries. To this end we used a TAMRA-labelled 32mer peptide with phosphorylation at Thr387 to mimic the p53 CTD that binds to the amphipathic groove of 14-3-3 monomers. Titration of 14-3-3σ to this peptide resulted in the expected increase in polarization and characteristic sigmoidal curve for a one site binding event (Fig. 2A, black). From this data an apparent K_d of 13.7 ± 1.8 μM could be extracted, in line with previously published values (FP, 14-3-3γ = 14.0 ± 3 μM [19]; ITC, 14-3-3σ = 16.3 μM [22]).

To unambiguously define an FP assay window suitable for the identification of both stabilizers and inhibitors of the interaction required both positive and negative control compounds are required. We

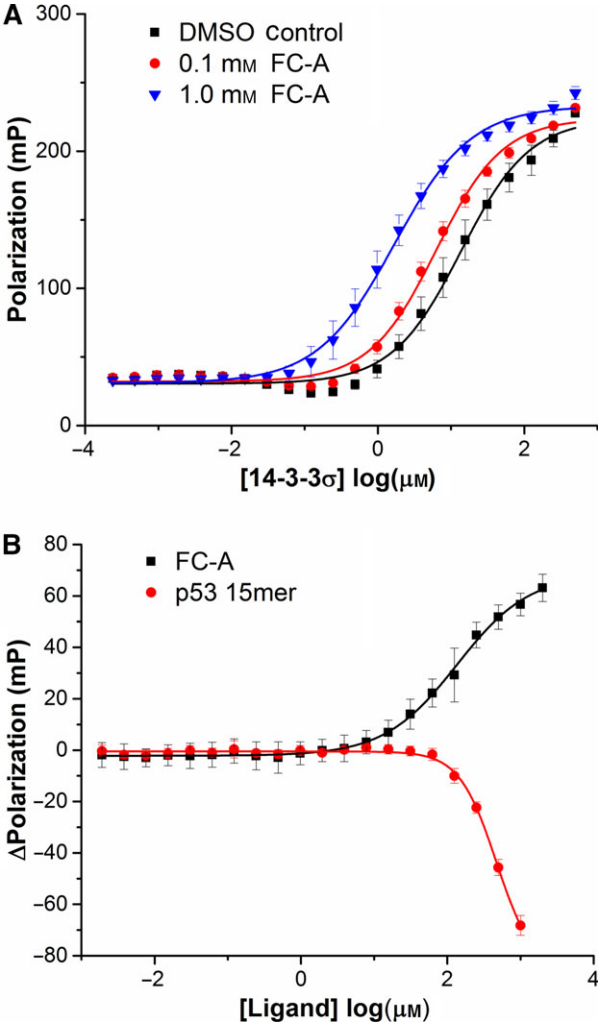

Fig. 2. FP experiments show FC-A stabilization. (A) 14-3-3σ titration to TAMRA-p53-CTD 32mer peptide (pThr387, 10 nM) in the presence of increasing concentrations of FC-A (0.00 mM, 0.10 mM, 1.0 mM). (B) Dose-response experiment showing change in polarization from the DMSO control (ΔPolarization) upon titration of FC-A and p53-CTD 15mer peptide (pThr387) to 14-3-3σ (10 μM) and TAMRA-p53-CTD 32mer peptide (pThr387, 10 nM). Data shown are mean ± SD of three separate experiments each with triplicate measurements.

therefore screened a narrow selection of potential modulators in single-shot format. It was envisaged that shorter, unlabelled peptides mimicking the p53 CTD (e.g. a 15mer peptide) or other 14-3-3 binding partners (e.g. ERα) [12] would likely compete for binding to 14-3-3 and thus prove to be ideal negative controls and indeed this was the case (see Fig. S1). No tool-compounds to probe for stabilization of this interaction had previously been reported and, as already discussed, it was not expected that other known 14-3-3 stabilizers would be effective at the unique binding

interface of p53. Never-the-less, in the interest of thoroughness we screened four fusicoccanes (FC-A, FC-A aglycone, FC-H-OMe [11] and FC-THF [14]) along with epibestatin, a synthetic 14-3-3 stabilizer [24] (see Fig. S1). To our surprise, FC-A showed a notable increase in polarization and intriguingly was the only fusicoccane screened to do so.

To confirm that the observed increase in polarization could be directly attributed to modulation of the interaction, 14-3-3σ was titrated to TAMRA-32mer in the presence of FC-A at two concentrations (Fig. 2A, red and blue). As the FC-A concentration increased the apparent K_ds were clearly reduced (indicating increased peptide affinity for protein) from 13.7 ± 1.8 μM in the absence of FC-A to 6.3 ± 0.6 μM at 0.10 mM FC-A and 1.7 ± 0.1 μM at 1.0 mM FC-A. Thus, albeit with relatively low potency FC-A (at 1.0 mM) induced an 8-fold stabilization of the 14-3-3σ interaction with the TAMRA-labelled p53 CTD peptide. Next, dose-response experiments were performed whereby FC-A and the p53 CTD 15mer peptide were titrated to fixed concentrations of 14-3-3σ and TAMRA-peptide. Here, FC-A showed a dose-dependent increase in polarization, further indicating genuine stabilization although with low potency: EC_{50} = 135 μM (±12 μM). A series of control experiments were also performed that ruled out changes in fluorescent intensity upon 14-3-3 and/or FC-A binding to the TAMRA labelled peptide being the reason for observed changes in polarization (see Fig. S1). Displacement of the TAMRA-peptide by 15mer p53 CTD peptide was also shown to be dose-dependent (Fig. 2B, red), although the IC_{50} value was found to be high and beyond the limits of accurate determination in this assay (IC_{50} > 200 μM).

Isothermal titration calorimetry confirms FC-A stabilization

In order to corroborate our FP findings thermodynamically we used ITC to compare binding of the unlabelled p53 CTD 15mer peptide to 14-3-3σ with and without FC-A. In the absence of FC-A the peptide was shown to bind 14-3-3σ with a K_d of 23.6 ± 2.2 μM (Fig. 3A) which again corresponded well to previously reported values (*vide supra*). In alignment with our FP analyses, the binding affinity was again enhanced in the presence of FC-A (1.0 mM) and the obtained K_d value was reduced to 5.40 ± 0.84 μM (Fig. 3B). In this experiment the factor of stabilization induced by FC-A was not as pronounced as that determined by FP: 4.5-fold stabilization c.f. 8-fold shown in FP. However, the values remain in the same order of magnitude and, whilst the two experiments are complimentary, the two K_ds obtained for different peptides cannot be directly compared. Control experiments showed no calorimetric changes when the same titrations were performed in the absence of 14-3-3σ protein (see Fig. S2).

The ITC data also revealed that a more negative enthalpy change (ΔH) upon peptide binding in the presence of FC-A is the significant contributing factor to a more negative ΔG and thus stabilization (-3657 cal·mol^{-1} c.f. -2807 cal·mol^{-1} in the control experiment; Fig. 3C). Although the entropic contribution is significant in both cases (indicating the importance of hydrophobic effects), there was no difference in the measured change in entropy (ΔS) between experiments with or without FC-A (Fig. 3C). These observations indicate a binding profile with more hydrogen bonding character in the ternary compared to binary system and no change in disorder between the two complexes. Thus, our ITC data (and FP experiments) provide compelling evidence for FC-A-induced enhancement of the affinity for p53 CTD peptides to 14-3-3σ.

Protein crystallography reveals paradoxical evidence

To gain structural insight into our biophysical observations we first sought an improved binary crystal structure that might reveal more electron density around the most C-terminal part of the p53 CTD peptide than was previously obtained [22]. Gratifyingly, a p53 CTD peptide consisting of the C-terminal 12 amino acid residues (including pThr387) in complex with 14-3-3σ yielded crystals that showed in-house diffraction to 1.8 Å resolution. The electron density obtained after molecular replacement allowed the building of all 12 C-terminal amino acid residues of the peptide (Fig. 4A). As expected, the phosphorylated threonine residue (pThr387) is seen to bind in the conserved basic pocket of the 14-3-3 amphipathic groove formed by Lys49, Arg56, Arg129 and Tyr130. The other residues also show good agreement with the previously reported structure [19]. Significantly, Glu388 is indeed observed to protrude into the proposed ligand binding pocket.

Although the three most C-terminal residues appear to be relatively flexible, as illustrated by an average B-factor of 43.7 Å^2 compared to 30.2 Å^2 for the whole peptide, a key feature of this novel binary structure is the clearly visible C-terminus forming a salt bridge with Arg60 of the 14-3-3σ protein. An explanation for the presence of the C-terminus in this structure and the lack thereof in our previously reported structure with the 9-mer peptide lies in the presence of Met384 in the 12-mer peptide. In the 9-mer structure Met384 and Lys382 of

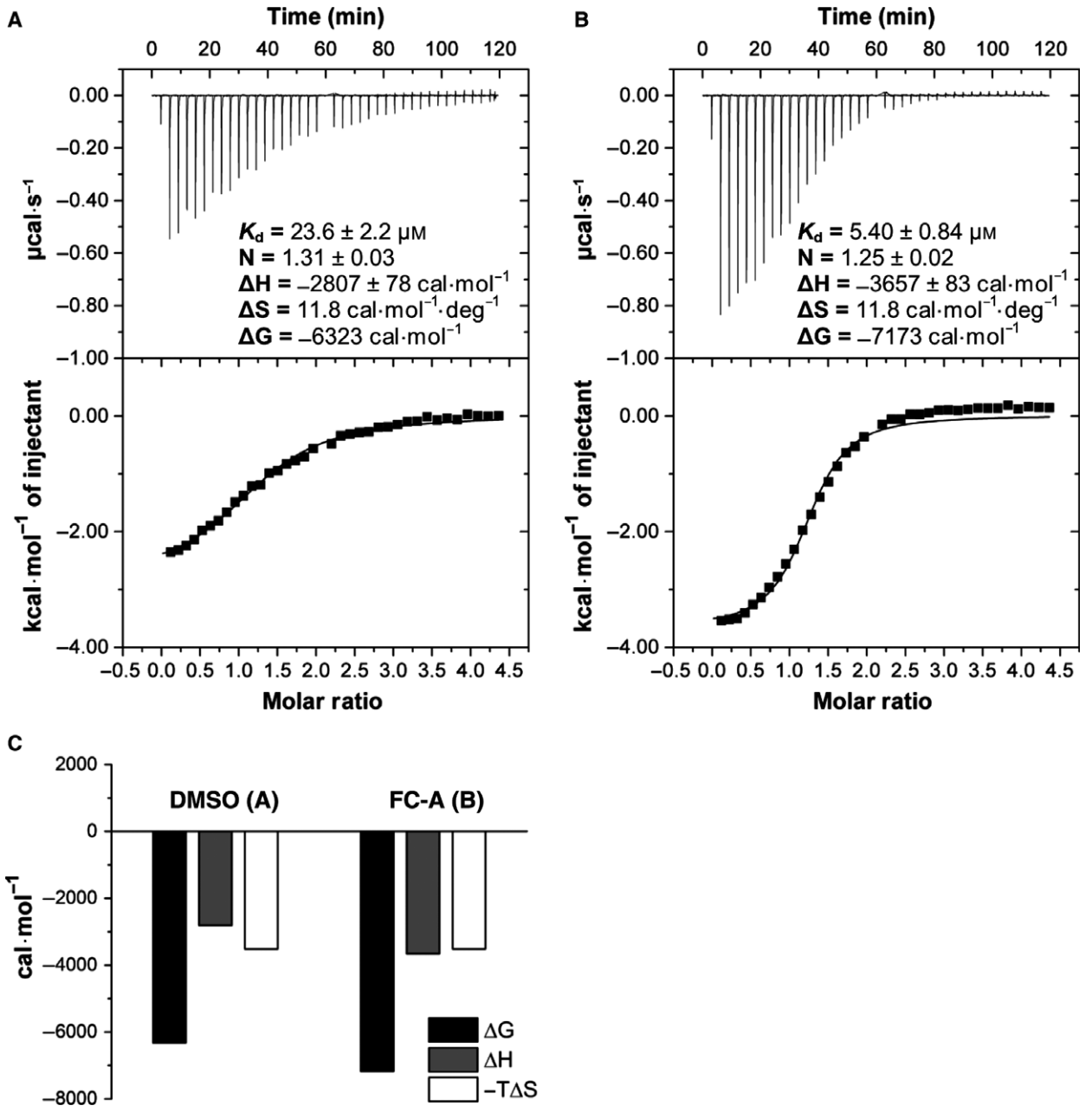

Fig. 3. ITC further confirms FC-A stabilization. p53-CTD 15mer peptide (pThr387, 1.0 mM syringe concentration) was titrated to 14-3-3σ (0.10 mM) in the presence of: (A) DMSO control; (B) 1.0 mM FC-A. (C) ΔH and $-T\Delta S$ contributions to ΔG. DMSO was used at 1% v/v throughout. Data are representative of three replicates (see Fig. S2).

p53 are not physically present and Arg60 of the 14-3-3 protein is seen to be flexible, adopting two conformations. In this structure this is not possible as the alternative Arg60 site is occupied by Met384 and Lys382 of the p53 peptide, forcing Arg60 to adopt a conformation pointing towards the p53 C-terminus.

To study the mode of stabilization of the p53 – 14-3-3σ complex by FC-A, we soaked the obtained crystals of the binary complex with FC-A. The soaked crystals were then measured at a synchrotron (PETRA III; DESY) and yielded diffraction to 1.2 Å resolution. After molecular replacement using the initial 12-mer structure we observed 14-3-3 in its expected fold and, crucially, additional electron density consistent with binding of FC-A. However, a large part of the electron density of the peptide was no longer observed, only

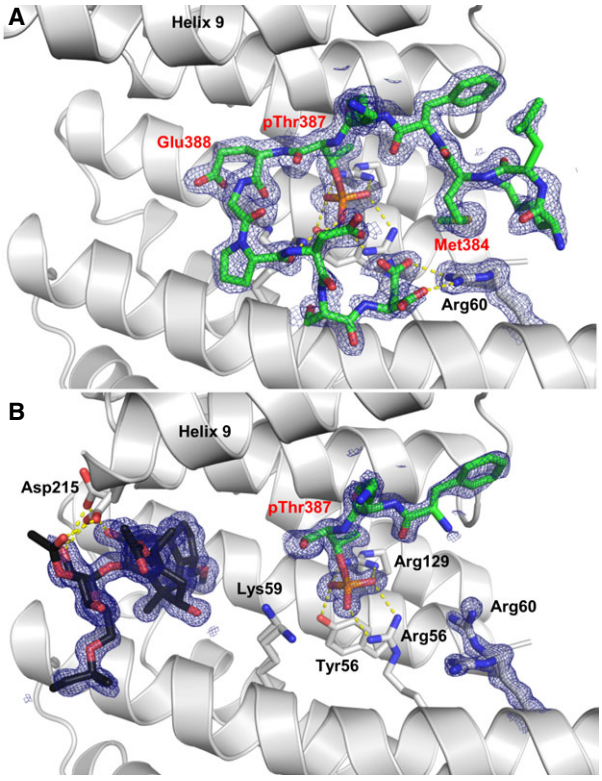

Fig. 4. (A) Binary crystal structure showing a p53-CTD 12mer peptide (pThr387, coloured according to atom with red residue labels) bound to 14-3-3σ (grey with black residue labels). 5MOC: wwpdb.org. (B) Ternary crystal structure showing a p53-CTD 12mer peptide (pThr387, coloured according to atom with red residue labels) bound to 14-3-3σ (grey with black residue labels) and FC-A (black). 5MXO: wwpdb.org.

allowing us to build in the key phosphorylated threonine pThr387 and two N-terminal amino acids (Fig. 4B). As a result, the C-terminus of the peptide is no longer visible and Arg60 of the protein is again observed to adopt two conformations. While there is some electron density where Glu388 would be expected, we were not able to build in any conformation of that amino acid, probably due to the presence of multiple peptide conformations required to accommodate binding of FC-A. Significantly, a shift in helix 9 common to other FC-A containing 14-3-3 crystal structures is observed [12,14]. The electron density in this region is difficult to interpret, but it is clear that the shift is driven by Asp215 of 14-3-3 making polar contacts with FC-A which is also consistent with previous crystal structures.

Discussion

In this communication we report the first example of small-molecule stabilization of the 14-3-3 – p53 PPI. Although FC-A is not selective for this 14-3-3 PPI and lacks the potency seen in systems with a 'mode 3' binding motif, it does represent a highly valuable tool-compound for further fundamental studies. The discovery also demonstrates the potential of this approach as a strategy to develop novel anti-cancer treatments and provides a useful starting point for rational drug design.

This study revealed an unusual paradox in the context of 14-3-3 PPI stabilization whereby biophysical and crystallographic data do not unambiguously corroborate each other. Our findings show a counter-intuitive relationship between biophysical and crystallographic experimental data. Whilst our biophysical data clearly point to FC-A-induced stabilization of the p53 – 14-3-3σ PPI, the crystal structure reveals a ternary structure with a highly disordered peptide binding partner compared to the binary structure. Therefore, if the crystallographic data was considered in isolation, it could be concluded that FC-A actually destabilizes the PPI interface. However this is not logical given that: First, the disorder observed in the ternary structure is not reflected in the ΔS values obtained by ITC which are unchanged between binary and ternary systems. Second, FC-A binding would not only need to compensate for the loss of key enthalpic contacts between the C-terminus of the p53 peptide and 14-3-3σ (as observed in the ternary structure) but also enhance the enthalpic contribution to binding as shown by the ΔH values obtained by ITC. Such a paradox might be explained by differing behaviour of the full length 14-3-3 construct used in our biophysical experiments compared to the truncated 14-3-3 ΔC construct used for crystallization. To investigate this we performed FP and ITC experiments with the truncated complex (see Fig. S3). In both cases this data mirrored the results obtained for the full length construct very closely and thus cannot explain these observations.

A likely explanation therefore is that the current crystal lattice does not allow the peptide to occupy its preferred conformation in the presence of FC-A. This artefactual result of crystal soaking would mean that the current data is not an accurate description of the ternary complex in solution. The data could also suggest that in this case stabilization is predominantly the result of a FC-A induced conformational change to 14-3-3 (i.e. the shift in helix 9 and that is common to other FC-A stabilized systems). This 'allosteric' rather than 'molecular glue' mode-of-action does not necessitate contact between FC-A and the p53 CTD peptide and thus might also explain the apparent disorder observed in the ternary structure. Ultimately, analysis of a ternary structure obtained by co-crystallization

would provide convincing evidence to prove one of these theories. However, despite significant efforts we have not yet been able to co-crystallize the ternary structure.

In conclusion, our results provide the first evidence that small-molecule stabilization of the p53 – 14-3-3 PPI is an interesting drug-discovery strategy that now warrants an expansive search for more potent and PPI-specific compounds. Our findings highlight the need for continued efforts to fully characterise the structural basis for p53 binding to 14-3-3 and stabilization of the interaction. With an improved and expanded chemical toolkit it will then be possible to test the viability of the stabilization approach in a cellular context.

Acknowledgements

This research is supported by funding from the European Union through the AEGIS project, H2020-MSCA-ITN-2015, grant number 67555 and H2020-MSCA IEF, grant number 705188 (RGD). We thank Loredana Spola, Joe Patel, Nathan Fuller, Heike Schönherr, and Robert Goodnow for various contributions in the perception and discussion of the project. We thank the team of beamline P11 of PETRAIII, DESY, Hamburg, Germany for help with data collection.

Author contributions

CO, HB, QC, AH, PC, and HC conceived the project and designed the experiments. RGD and AK prepared the peptides and conducted the FP and ITC experiments. SA and SL carried out the crystallography experiments and SA performed the data analysis. RGD, SA, HB, HC and CO wrote the manuscript.

References

1 Vousden KH and Prives C (2009) Blinded by the light: the growing complexity of p53. *Cell* **137**, 413–431.
2 Khoo KH, Hoe KK, Verma CS and Lane DP (2014) Drugging the p53 pathway: understanding the route to clinical efficacy. *Nat Rev Drug Discov* **13**, 217–236.
3 Lambert JMR, Gorzov P, Veprintsev DB, Söderqvist M, Segerbäck D, Bergman J, Fersht AR, Hainaut P, Wiman KG and Bykov VJN (2009) PRIMA-1 reactivates mutant p53 by covalent binding to the core domain. *Cancer Cell* **15**, 376–388.
4 Joerger AC and Fersht AR (2016) The p53 pathway: origins, inactivation in cancer, and emerging therapeutic approaches. *Annu Rev Biochem* **85**, 375–404.
5 Joerger AC, Bauer MR, Wilcken R, Baud MGJ, Harbrecht H, Exner TE, Boeckler FM, Spencer J and Fersht AR (2015) Exploiting transient protein states for the design of small-molecule stabilizers of mutant p53. *Structure* **23**, 2246–2255.
6 Yu X, Narayanan S, Vazquez A and Carpizo DR (2014) Small molecule compounds targeting the p53 pathway: are we finally making progress? *Apoptosis* **19**, 1055–1068.
7 Tinti M, Madeira F, Murugesan G, Hoxhaj G, Toth R and Mackintosh C (2014) ANIA: annotation and integrated analysis of the 14-3-3 interactome. *Database (Oxford)* **2014**, bat085.
8 Aghazadeh Y and Papadopoulos V (2016) The role of the 14-3-3 protein family in health, disease, and drug development. *Drug Discov Today* **21**, 278–287.
9 Bartel M, Schäfer A, Stevers LM and Ottmann C (2014) Small molecules, peptides and natural products: getting a grip on 14-3-3 protein-protein modulation. *Future Med Chem* **6**, 903–921.
10 Hartman AM and Hirsch AKH (2017) Molecular insight into specific 14-3-3 modulators: inhibitors and stabilisers of protein–protein interactions of 14-3-3. *Eur J Med Chem* **136**, 573–584.
11 de Boer AH and de Vries-van Leeuwen IJ (2012) Fusicoccanes: diterpenes with surprising biological functions. *Trends Plant Sci* **17**, 360–368.
12 De Vries-van Leeuwen IJ, da Costa Pereira D, Flach KD, Piersma SR, Haase C, Bier D, Yalcin Z, Michalides R, Feenstra KA, Jiménez CR *et al.* (2013) Interaction of 14-3-3 proteins with the estrogen receptor alpha F domain provides a drug target interface. *Proc Natl Acad Sci USA* **110**, 8894–8899.
13 Camoni L, Di Lucente C, Visconti S and Aducci P (2011) The phytotoxin fusicoccin promotes platelet aggregation via 14-3-3–glycoprotein Ib-IX-V interaction1. *Biochem J* **436**, 429–436.
14 Anders C, Higuchi Y, Koschinsky K, Bartel M, Schumacher B, Thiel P, Nitta H, Preisig-Müller R, Schlichthörl G, Renigunta V *et al.* (2013) A semisynthetic fusicoccane stabilizes a protein-protein interaction and enhances the expression of K+ channels at the cell surface. *Chem Biol* **20**, 583–593.
15 Stevers LM, Lam CV, Leysen SFR, Meijer FA, van Scheppingen DS, de Vries RMJM, Carlile GW, Milroy LG, Thomas DY, Brunsveld L *et al.* (2016) Characterization and small-molecule stabilization of the multisite tandem binding between 14-3-3 and the R domain of CFTR. *Proc Natl Acad Sci USA* **113**, E1152–E1161.
16 Bier D, Bartel M, Sies K, Halbach S, Higuchi Y, Haranosono Y, Brummer T, Kato N and Ottmann C (2016) Small-molecule stabilization of the 14-3-3/Gab2 protein-protein interaction (PPI) interface. *ChemMedChem* **11**, 911–918.

17 Molzan M, Kasper S, Röglin L, Skwarczynska M, Sassa T, Inoue T, Breitenbuecher F, Ohkanda J, Kato N, Schuler M *et al*. (2013) Stabilization of physical RAF/14-3-3 interaction by cotylenin A as treatment strategy for RAS mutant cancers. *ACS Chem Biol* **8**, 1869–1875.
18 Yang H-Y, Wen Y-Y, Chen C-H, Lozano G and Lee M-H (2003) 14-3-3 Sigma positively regulates P53 and suppresses tumor growth. *Mol Cell Biol* **23**, 7096–7107.
19 Rajagopalan S, Jaulent AM, Wells M, Veprintsev DB and Fersht AR (2008) 14-3-3 activation of DNA binding of p53 by enhancing its association into tetramers. *Nucleic Acids Res* **36**, 5983–5991.
20 Rajagopalan S, Sade RS, Townsley FM and Fersht AR (2010) Mechanistic differences in the transcriptional activation of p53 by 14-3-3 isoforms. *Nucleic Acids Res* **38**, 893–906.
21 Chen DY, Dai DF, Hua Y and Qi WQ (2015) p53 suppresses 14-3-3γ by stimulating proteasome-mediated 14-3-3γ protein degradation. *Int J Oncol* **46**, 818–824.
22 Schumacher B, Mondry J, Thiel P, Weyand M and Ottmann C (2010) Structure of the p53 C-terminus bound to 14-3-3: implications for stabilization of the p53 tetramer. *FEBS Lett* **584**, 1443–1448.
23 Huang EY, Wang FS, Chen YM, Chen YF, Wang CC, Lin IH, Huang YJ and Yang KD (2014) Amifostine alleviates radiation-induced lethal small bowel damage via promotion of 14-3-3sigma-mediated nuclear p53 accumulation. *Oncotarget* **5**, 9756–9769.
24 Rose R, Erdmann S, Bovens S, Wolf A, Rose M, Hennig S, Waldmann H and Ottmann C (2010) Identification and structure of small-molecule stabilizers of 14-3-3 protein-protein interactions. *Angew Chem Int Ed* **49**, 4129–4132.

Supporting information

Additional Supporting Information may be found online in the supporting information tab for this article:

Data S1. Experimental procedures.

Fig. S1. Fluorescence polarization supporting information.

Fig. S2. (A, B) Replicate ITC experiments where Experiment 1 is shown in Fig. 3 (main text). 15mer peptide (1.0 mM syringe concentration) was titrated to 14-3-3σ (0.1 mM) in the presence of: (A) DMSO control; (B) 1.0 mM FC-A. (C) Control experiments where p53 CTD 15mer peptide (1.0 mM) was titrated to buffer in the presence of DMSO or 1 mM FC-A. DMSO was used at 1% v/v throughout. Further experimental details can be found in the Data S1.

Fig. S3. Experiments performed with the 14-3-3σ ΔC construct.

Fig. S4. LC-MS analysis of the 15mer peptide prepared in-house.

Table S1. Crystallography data and refinement statistics for 5MOC and 5MXO.